Flow-Induced Draping

Lionel Schouveiler* and Christophe Eloy

Aix Marseille Université, CNRS, Centrale Marseille, IRPHE UMR 7342, F-13384 Marseille, France

(Received 8 February 2013; revised manuscript received 24 June 2013; published 9 August 2013)

Crumpled paper or drapery patterns are everyday examples of how elastic sheets can respond to external forcing. In this Letter, we study experimentally a different sort of forcing. We consider a circular flexible plate clamped at its center and subject to a uniform flow normal to its initial surface. As the flow velocity is gradually increased, the plate exhibits a rich variety of bending deformations: from a cylindrical shape, to isometric developable cones with azimuthal periodicity two or three, to eventually a rolled-up period-three cone. We show that this sequence of flow-induced deformations can be qualitatively predicted by a linear analysis based on the balance between elastic energy and pressure force work.

DOI: 10.1103/PhysRevLett.111.064301 PACS numbers: 46.40.Jj, 46.70.De

Bending and stretching are the two deformation modes of thin elastic plates. For plates of thickness h and typical length R, the ratio between bending and stretching energies scales as $(h/R)^2$. As a result, in the limit $h \ll R$ and if the boundary conditions enable it, thin plates will bend rather than stretch. For instance, a suspended piece of fabric generally exhibits draperies that have a conical shape. These particular deformations are isometric almost everywhere; i.e., the surface is not stretched or compressed compared to its initial state. In this example, the fold number and size are determined by the competition between gravity and elasticity [1] and stretching is focused in a small area in the vicinity of the cone tip. Such conical singularities are referred to as a d cone, for "developable cone." They are one of the two kinds of elementary singularities in thin plate deformations, the other being ridges, in which stretching is focused along lines. These two elementary singularities can be visualized by unfolding a sheet of crumpled paper: they appear respectively as crescent- or linelike permanent marks and result from plastic deformations of the paper [2].

Developable cones have been the subject of specific theoretical analyses [3], as well as experiments consisting generally in pushing a flat elastic plate into a ring [4,5]. In addition to crumpled paper and gravity-induced draperies, d cones have also been reported in delamination processes [6], tissue growth [7], and in suspended thin layers of viscous fluid [8]. In this Letter, we propose an experiment in which d cones are induced by flow-induced loads on a thin elastic plate. In this experimental setup, a rich variety of deformations can be observed: cylindrical shapes, d cones with two- or threefold azimuthal symmetries, and a threefold cone that is itself folded, thereby breaking the azimuthal periodicity.

The deformation of thin flexible structures due to flow-induced loads has been investigated in the past as a possible strategy to reduce the drag, comparatively to rigid structures [9–11]. This phenomenon has been particularly observed for plants that adopt more streamlined shapes to withstand high winds or water currents [12,13]. For instance, tulip trees have broad leaves that can reconfigure into cones, thus allowing them to reduce their drag and resist breakage [14]. This particular reconfiguration has motivated analytical [15] as well as experimental [16] studies that have considered circular flexible plates cut along one radius, clamped at their center, and placed in a uniform flow. These plates have been shown to roll up into circular cones whose angle become sharper as the flow velocity is increased.

In the present study, experiments are performed with circular polysiloxane plates of thickness $h = 6 \times 10^{-4}$ m, bending rigidity $B = 1.8 \times 10^{-4}$ N m, density $\rho_p = 1200$ kg m^{-3}, and variable radius R in the interval $0.02 < R < 0.1$ m. The plate is attached at its center to an upstream elbow and held in a low-turbulence horizontal water channel of 0.38 m $\times$ 0.45 m test section (Fig. 1). This water channel can produce a uniform flow of velocity U perpendicular to the plane that initially contains the plate. The flow velocity can be varied up to 1 m s^{-1}, with fluctuations below 1%.

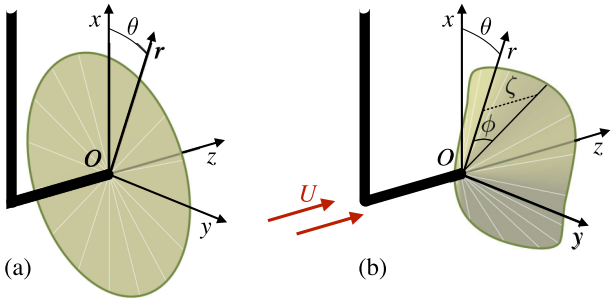

FIG. 1 (color online). Experimental setup. A flexible circular plate is clamped onto an elbow (a). When placed in a uniform water flow of velocity U, the plate deforms (b). The function $\phi(\theta)$ describes the d cone deformation of the plate.

A typical experiment consists, for a given plate of radius R, of gradually increasing the flow velocity starting from $U = 0$. As the plate deforms due to flow-induced loads, it is imaged through the transparent channel walls, both along the y and z axes (Fig. 1). For each plate radius studied, the sequence of deformation modes is identical. At small flow velocities, the plate bends around one of its diameters forming a cylindrical surface with generatrices perpendicular to the incoming flow [Fig. 2(a)]. This mode has been called "mode C," for cylindrical. This sort of bending deformation has been studied in the literature with rectangular plates placed in a uniform flow [11], or, in a two-dimensional geometry, with flexible filaments placed into a flowing soap film [9,10].

For larger flow velocities, different draping modes appear. These draping patterns are shown in Figs. 2(b)–2(d). They have a conical shape that can be analytically described by the angle $\phi(\theta)$ (Fig. 1). When the flow velocity reaches a first threshold, the plate reconfigures continuously from its initial cylindrical shape into a cone with $n = 2$ folds [Fig. 2(b)]. After a second threshold, the plate exhibits $n = 3$ folds [Fig. 2(c)]. In some experiments, the two- and threefold modes can coexist intermittently on an interval of flow velocities. Both of these deformations are azimuthally periodic such that the function $\phi(\theta)$ has a period $2\pi/n$. This periodicity is lost beyond the last threshold. The last deformation mode still presents three folds but these folds are themselves "rolled up" or pushed against each other, breaking the periodicity [Fig. 2(d)]. This last mode persists up to the highest flow velocity explored during the present study (i.e., $U = 1\ \mathrm{m\,s^{-1}}$). These conical modes, which appear in sequential order after the "mode C," are called mode $2F$, mode $3F$, and mode $3F^*$, respectively. Note that, although the elbow maintaining the plate in the flow induces a breaking of the azimuthal symmetry, the azimuthal phase of the different modes presented in Figs. 2(a)–2(d) is arbitrary and has been observed to change when repeating the experiments.

To assess the influence of the plate radius on the velocity thresholds, different experiments have been conducted with different radii for $0.02 < R \leq 0.1$ m. Qualitatively, the larger the plate radius, the smaller the thresholds. The domains of observation of the four deformation modes in the plane U-R are reported in a morphological diagram (Fig. 3). This diagram corresponds to experiments performed when the velocity U is gradually increased. Note that, when the flow velocity is decreased, the reverse sequence of modes can be observed (i.e., modes $3F^*$, $3F$, $2F$, and C), but the velocity thresholds are systematically lower than for increasing velocities, revealing hysteresis loops. These hysteresis loops can be as large as 50% of the velocity thresholds and are likely due to energetic barriers between modes (see the Supplemental Material [17]).

To gain better insight into the sequence of draping modes observed in experiments, we now consider the energy associated with the flow-induced deformations. For this purpose, we consider a thin circular sheet of bending rigidity B, radius R, area S, and thickness h that initially lies in the plane $z = 0$. When subject to a flow of density ρ and velocity U in the z direction, this sheet deforms into a conical surface, such that the streamwise plate deflection can be written $\zeta(r, \theta) = rf(\theta)$, where (r, θ, z) are the cylindrical coordinates with the origin O at the

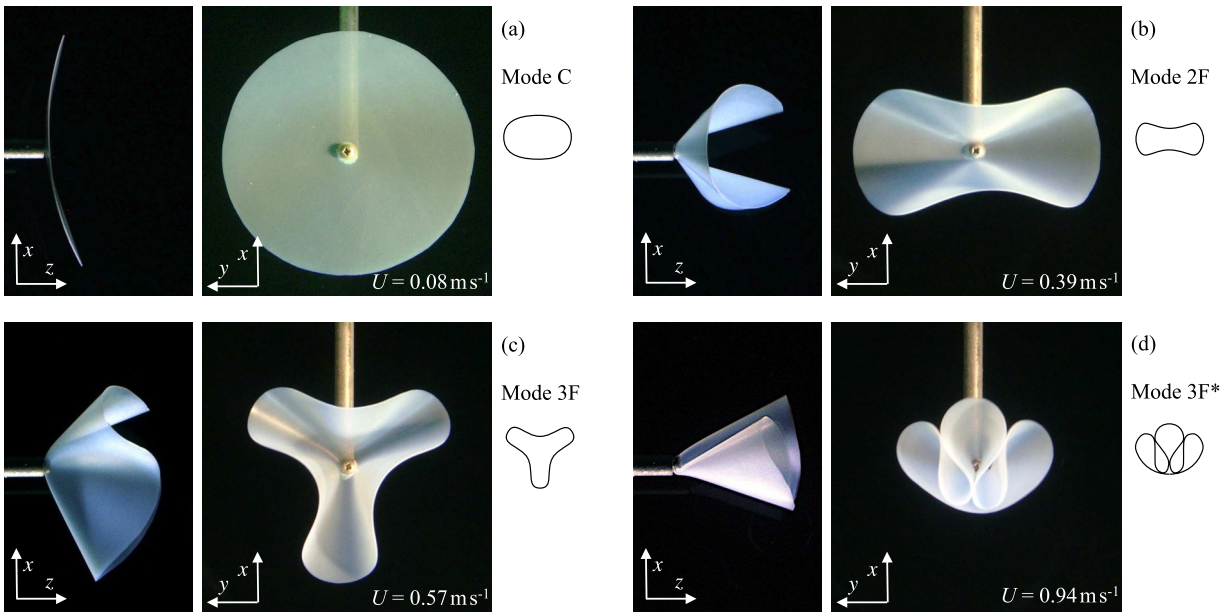

FIG. 2 (color online). Draping modes of a circular plate of radius $R = 0.05$ m. When the flow velocity is gradually increased, different draping patterns become visible starting from "mode C," a cylindrical mode (a), to "mode $2F$," a twofold conical mode (b), "mode $3F$," a threefold mode (c), and eventually "mode $3F^*$," a bent threefold mode (d).

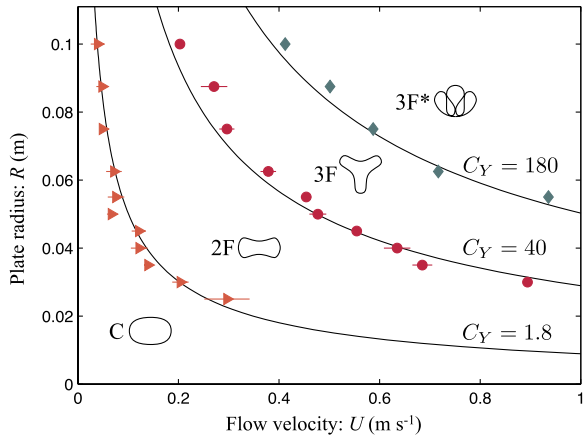

FIG. 3 (color online). Morphological diagram in the U-R plane. The symbols mark the transitions, as the flow velocity is increased, between the different modes pictured. The error bars on the triangles, associated to the $C \rightarrow 2F$ transition, correspond to a continuous transition, while the error bars of the $2F \rightarrow 3F$ transition (circles) correspond to an intermittent coexistence of the two modes. The solid lines are isovalues of the Cauchy number as defined in Eq. (3).

cone tip (Fig. 1). The function $f(\theta)$ describes the conical modes such that $f(\theta) = \tan\phi(\theta)$.

In this problem, a Reynolds number, $\mathrm{Re} = UR/\nu$, can be defined, which compares inertia to viscous forces, with ν the kinematic viscosity of the fluid. This Reynolds number being of the order of 10^5, viscous effects can be neglected here. Since buoyancy can also be neglected because the plate material has almost the same density as water, the total energy of the plate $\mathcal{E}$ is the difference between its elastic energy and the potential energy corresponding to the work done by the pressure forces. In the asymptotic limit of thin plates ($h/R \ll 1$), we will assume that the plate undergoes pure bending almost everywhere such that its elastic energy is dominated by bending energy,

$$\mathcal{E}_b = \frac{B}{2}\int_S (\Delta\zeta)^2 dS = \frac{B}{2}\ln\frac{R}{R_c}\int_0^{2\pi}(f + f'')^2 d\theta, \quad (1)$$

where $\Delta\zeta = (f + f'')/r$ is the local curvature of the plate and primes denote derivatives with respect to θ. The cutoff radius R_c in Eq. (1) comes from the logarithmically divergent integral as r goes to 0. Physically this means that pure bending deformations cannot persist up to the cone tip ($r = 0$). Around the tip, in a region of typical size $R_c \ll R$, stretching cannot be neglected anymore. Yet, the precise value of R_c is not crucial since the bending energy $\mathcal{E}_b$ varies only logarithmically with R_c.

The work done by the fluid pressure when the plate deforms into a cone can be evaluated as

$$\mathcal{E}_p = \int_S \int_0^{\phi} p r d\varphi dS, \quad (2)$$

where p is the local pressure jump across the plate. With the assumptions made above, a dimensionless number can be defined, which compares the typical work done by pressure forces ($\rho U^2 R^3$) to the typical bending energy ($B\ln(R/R_c)$). This elastohydrodynamic number is a Cauchy number and can be written as

$$C_Y = \frac{\rho U^2 R^3}{B\ln(R/R_c)}, \quad (3)$$

with $\rho = 1000\ \mathrm{kg\,m^{-3}}$ the density of water. This Cauchy number is the only dimensionless number of the problem; it has been varied on almost 6 orders of magnitude in the experiments ($0.003 < C_Y < 1800$). Isovalues of C_Y are reported on the morphological diagram in Fig. 3 and it shows that the experimentally measured thresholds all correspond to a fixed value of C_Y. The transition between modes C and $2F$ occurs at $C_Y \approx 1.8$, while transition between modes $2F$ and $3F$ appears at $C_Y \approx 40$, and the one between $3F$ and $3F^*$ at $C_Y \approx 180$.

To go further, we have calculated the energy associated with linear draping modes with azimuthal wave numbers $n = 2$, 3, and 4 (noted $2F$, $3F$, and $4F$ by analogy with the experimentally observed modes). In the limit of small deflections, the developability condition reads $\int_0^{2\pi}(f^2 - f'^2)d\theta = 0$ [2]. The simplest conical surfaces with azimuthal wave number n that satisfy this condition are given by $f(\theta) = f_0(1 + \sqrt{2/(n^2-1)}\sin n\theta)$ where f_0 is a small amplitude [3,8]. To evaluate the pressure jumps associated with these deformations, we assumed that the pressure is constant along a generatrix of the conical shape and is equal to the pressure on a circular cone of same angle as determined in Ref. [16] using momentum conservation arguments. It yields a pressure jump, $p = \rho U^2(1 - \sin\phi)$.

To calculate the total energy of cylindrical deformations (mode C), we assumed a constant curvature everywhere on the plate, and a pressure jump, $p = \rho U_n^2$, with U_n the component of the flow velocity normal to the plate surface. Note that, in order to compare cylindrical mode (for which there is no stretching) and conical modes (for which stretching is localized in a zone of size R_c), we used $\ln(R/R_c) = 4$. This value has been considered as a fitting parameter and corresponds to $R_c \approx 1$ mm, which is approximately the diameter of the central hole in the plate.

For a given mode, C, $2F$, $3F$, or $4F$, and a given Cauchy number, we can thus calculate numerically the deformation amplitude that minimizes the total energy $\mathcal{E} = \mathcal{E}_b - \mathcal{E}_p$. We can then compare these energies, as the Cauchy number is increased (Fig. 4). According to this analysis, the modes that minimize the energy follow the same sequence as in the experiments: mode C for $C_Y < 4.6$, mode $2F$ for $4.6 < C_Y < 318$, and mode $3F$ for $C_Y > 318$ [18]. However, the values of these thresholds are different from experimental observations (Fig. 3). The discrepancy is probably due to the rather crude modeling of the pressure work, the assumption of linear deflections, or the absence of stretching energy in the budget. Note that the mode with

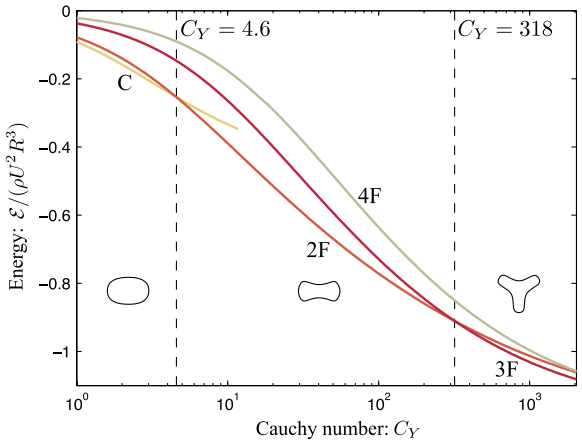

FIG. 4 (color online). Energy as a function of the Cauchy number for the modes C, $2F$, $3F$, and $4F$. These energies are found by minimizing the total energy $\mathcal{E}$ when the deformation amplitude is varied. The calculation for mode C is stopped when the radius of curvature reaches $2R/\pi$.

azimuthal wave number $n = 4$ never has the lowest energy, whatever the value of the Cauchy number. And indeed, in the experiments, even when we tried to force a fourfold mode by hand, the system always returned to its spontaneous two- or threefold mode.

The above approach does not allow one to model the complex deformations of the mode $3F^*$ observed for the largest values of C_Y. However, for this mode, a qualitative explanation can be provided. On the one hand, we note that the mode $3F^*$ is formed of three folds that are grouped whereas they are arranged periodically along the azimuthal direction for the mode $3F$. Therefore the bending energy of the mode $3F^*$ is probably only slightly larger than its $3F$ counterpart. On the other hand, during the process of grouping, the area swept by the three peripheral folds is important, and, as a consequence, yields a substantial work of the pressure forces. For large flow velocities, the importance of pressure work becomes relatively more important, and the mode $3F^*$ becomes favored compared to the mode $3F$.

It should be stressed that the sequence of modes observed in the present study is different from gravity-induced draping [1,8]. When the external force driving the plate deformation is the weight, d cones of an increasingly large number of folds are observed as the plate radius is increased. Additionally, the mode $3F^*$ is never observed. This can be qualitatively understood by noting that the weight exerts a force that is always parallel to the z axis, thus providing no favorable work during the wrapping process characteristic of the mode $3F^*$. On the contrary, pressure forces are normal to the surface and can thus provide such a favorable work.

In summary, we have studied how a circular flexible sheet deforms when subject to flow-induced loads. A sequence of four deformation modes has been evidenced. For low flow velocities, the sheet deforms cylindrically, while draping patterns appear for larger flow velocities. In this latter case, the sheet deforms into d cones of different azimuthal symmetries. As the flow velocity is increased, a periodic twofold mode is first observed, then a periodic threefold mode, and eventually a nonperiodic threefold mode. The transition between the first three modes has been predicted using a linear model based on energetic arguments and a qualitative explanation has been proposed to explain why the azimuthal symmetry is eventually lost for the largest flow velocities. In addition, we showed that the only parameter that governs the transition between modes is the dimensionless Cauchy number, in agreement with experimental observations.

We warmly thank N. Vandenberghe for his help with the fabrication of plates and A. Boudaoud for insightful comments. C. E. acknowledges support from the European Union (PIOF-GA-2009-252542).

*lionel@irphe.univ-mrs.fr

[1] E. Cerda, L. Mahadevan, and J. M. Pasini, Proc. Natl. Acad. Sci. U.S.A. **101**, 1806 (2004).
[2] B. Audoly and Y. Pomeau, *Elasticity and Geometry* (Oxford University Press, New York, 2010).
[3] M. Ben Amar and Y. Pomeau, Proc. R. Soc. A **453**, 729 (1997).
[4] E. Cerda and L. Mahadevan, Phys. Rev. Lett. **80**, 2358 (1998).
[5] S. Chaïeb, F. Melo, and J. C. Géminard, Phys. Rev. Lett. **80**, 2354 (1998).
[6] J. Chopin, D. Vella, and A. Boudaoud, Proc. R. Soc. A **464**, 2887 (2008).
[7] J. Dervaux and M. Ben Amar, Phys. Rev. Lett. **101**, 068101 (2008).
[8] A. Boudaoud and S. Chaïeb, Phys. Rev. E **64**, 050601 (2001).
[9] S. Alben, M. Shelley, and J. Zhang, Nature (London) **420**, 479 (2002).
[10] S. Alben, M. Shelley, and J. Zhang, Phys. Fluids **16**, 1694 (2004).
[11] F. Gosselin, E. de Langre, and B. A. Machado-Almeida, J. Fluid Mech. **650**, 319 (2010).
[12] S. Vogel, *Life in Moving Fluids* (Princeton University Press, Princeton, NJ, 1994).
[13] E. de Langre, A. Gutierrez, and J. Cossé, C.R. Mécanique **340**, 35 (2012).
[14] S. Vogel, J. Exp. Bot. **40**, 941 (1989).
[15] S. Alben, Phys. Fluids **22**, 081901 (2010).
[16] L. Schouveiler and A. Boudaoud, J. Fluid Mech. **563**, 71 (2006).
[17] See Supplemental Material at http://link.aps.org/supplemental/10.1103/PhysRevLett.111.064301 for additional results on the hysteresis of the transitions, and with different materials.
[18] The value chosen for cutoff radius R_c affects the threshold between the C and $2F$ modes, but not the threshold between the $2F$ and $3F$ modes.